

Document downloaded from:

<http://hdl.handle.net/10251/156934>

This paper must be cited as:

Iglesias-Martínez, ME.; Fernández De Córdoba, P.; Antonino Daviu, JA.; Conejero, JA. (2019). Detection of nonadjacent rotor faults in induction motors via spectral subtraction and autocorrelation of stray flux signals. IEEE Transactions on Industry Applications. 55(5):4585-4594. <https://doi.org/10.1109/TIA.2019.2917861>



The final publication is available at

<https://doi.org/10.1109/TIA.2019.2917861>

Copyright Institute of Electrical and Electronics Engineers

Additional Information

(c) 2019 IEEE. Personal use of this material is permitted. Permission from IEEE must be obtained for all other uses, in any current or future media, including reprinting/republishing this material for advertising or promotional purposes, creating new collective works, for resale or redistribution to servers or lists, or reuse of any copyrighted component of this work in other works.

# Detection of Nonadjacent Rotor Faults in Induction Motors via Spectral Subtraction and Autocorrelation of Stray Flux Signals

Miguel E. Iglesias-Martínez, Pedro Fernández de Córdoba, Jose A. Antonino-Daviu,  
*IEEE Senior Member*, and J. Alberto Conejero

**Abstract** – In this paper, statistical signal processing techniques are applied to electromotive force signals captured in external coil sensors for adjacent and nonadjacent broken bars detection in induction motors. An algorithm based on spectral subtraction analysis is applied for broken bar identification, independent of the relative position of the bar breakages. Moreover, power spectrum analyses enable the discrimination between healthy and faulty conditions.

The results obtained with experimental data prove that the proposed approach provides good results for fault detectability. Moreover the identification of the faults, and the signal correlation indicator to prove the results, are also presented for different positions of the flux sensor.

**Index Terms**— Fault Diagnosis; Induction Motors; Flux; Signals; Spectral Analysis.

## I. INTRODUCTION

A recent trend in the electric motor condition monitoring area relies on combining the information obtained from the analyses of different machine quantities (currents, vibrations, temperatures, etc...) to reach a more reliable conclusion about its health. This is due to the fact that it has been proven that the analysis of a single quantity enables to diagnose specific faults or anomalies but it is not enough to determine the health of the whole motor. In this context, the analysis of classical quantities that are well-known in the industry, such as currents or vibrations, has shown some problems or drawbacks for the diagnosis of certain faults [1].

With regards to the condition of the rotor, neither current nor vibration analyses have proven to be valid in all the cases that may rise in industry; it has been reported, for instance, the occasional occurrence of false indications when these techniques are used [2]-[5]. One of the cases where these techniques have not shown good results when detecting rotor

damages is under the presence of nonadjacent bar breakages in the rotor cage. In this regard, over recent decades, several works have reported problems of current-based techniques to detect such fault: in the early 80's Hargis *et al.* already pointed out that when the broken bars are separated by  $\pi/2$  electrical radians, current analysis may underestimate the number of broken bars and may even fail to detect the defect [6]. Years later, Benbouzid [7] ratified the previous statement, remarking that the lower sideband harmonic (LSH) may not be discernible when the breakages occur at specific relative locations. The statement of the problem led several authors to deepen in the physical study of the phenomenon by developing suitable electric motor models that were aimed to analyze the relation between the relative positions of the broken bars and the results of *Motor Current Signature Analysis* (MCSA). This is the case of [8], in which a model of a 22-bar, four-pole machine was built considering all the potential cases of double breakages; the authors concluded again that the amplitude of the LSH greatly depends on the relative position between the broken bars. Other physical analyses of the problem that reached analogous conclusions can be found in [9]-[10], while empirical analyses were performed in [11]. Finally, in [12] it is presented a physical analysis of the air gap magnetic anomaly for the case of any double bar breakage, including multiple experimental tests that confirmed the effect of the bar breakage location on the MCSA results. This work proved that when two broken bars are separated by a distance equal to half the pole pitch, the LSH amplitude can be significantly lower than that reached for the case of only one broken bar.

In spite of the number of works dealing with the nonadjacent broken bars issue, note that most of them are focused on presenting rigorous analyses of the problem which ratify the difficulties of classical diagnosis methods. However, none of the previous works has proposed reliable solutions to the problem, neither based on current analysis nor on analysis of other quantities. More recently, several groups of authors have proposed novel strategies that were intended to solve the nonadjacent broken bars diagnosis issue. In this regard, [13] proposed a method for detecting nonadjacent bar breakages, which relies on the study, both at steady-state and under starting, of high order harmonics (located at  $f \cdot (5-4 \cdot s)$  and  $f \cdot (5-6 \cdot s)$ , with  $f$ =supply frequency and  $s$ =slip) produced by the fault in the stator current. The problem of this approach is that these harmonics often have low amplitudes and are not always easily discernible neither

---

This work was supported in part by MEC, Project MTM 2016-7963-P and in part by the Spanish 'Ministerio de Ciencia Innovación y Universidades' and FEDER program in the framework of the 'Proyectos de I+D de Generación de Conocimiento del Programa Estatal de Generación de Conocimiento y Fortalecimiento Científico y Tecnológico del Sistema de I+D+i, Subprograma Estatal de Generación de Conocimiento' (ref: PGC2018-095747-B-I00).

Miguel E. Iglesias Martínez is with Universidad de Pinar del Río Hermanos Saíz Montes de Oca, Departamento de Telecomunicaciones, Martí 270, Pinar del Río, CUBA (e-mail: migueliglesias2010@gmail.com).

Pedro Fernández de Córdoba and J. Alberto Conejero are with the Instituto Universitario de Matemática Pura y Aplicada, Universitat Politècnica de València, E-46022 Valencia, SPAIN (e-mails: pfernandez@mat.upv.es, aconejero@upv.es).

Jose A. Antonino-Daviu is with the Instituto Tecnológico de la Energía, Universitat Politècnica de València, E-46022 Valencia, SPAIN (e-mail: joanda@die.upv.es).

on the Fourier spectrum of the steady-state current nor on the time-frequency analysis of the starting current. On the other hand, [14] compares the performance of MCSA and *Zero Sequence Current (ZSC)* analysis to detect both adjacent and nonadjacent bars. This work concludes that the ZSC analysis may be promising to avoid potential false negative indications of MCSA. However, this method requires the measurement of currents in all three motor phases (in delta configuration) for the later computation of the ZSC, which is not easy in many real industrial applications. In a more recent work, Gyftakis *et al* [15] proposed a reliable indicator to detect nonadjacent broken bars based on the *Filtered Park's/Extended Park's Vector Approach (FPVA/FEPVA)*. This method relies on monitoring the higher harmonic index of the Park's vector. Their results were confirmed via multiple experimental tests. Once again, the problem is that measurement of all three currents is necessary, a requirement that may significantly complicate the industrial applicability of the approach.

Due to the important problems of the methods relying of current analysis to detect nonadjacent broken bars, other technologies based on alternative quantities are being explored. In this context, in [16] it is proposed the installation of a Hall effect sensor between two stator slots and the subsequent *Fast Fourier Transform (FFT)* analysis of the registered data. The disadvantage of this method, which proves to be effective under low slip operating conditions, is the unpractical nature of the approach due to the necessity of sensor installation during motor assembly. However, this work demonstrates the potential of the flux analysis for such diagnosis, even though it is focused on the analysis of the internal flux in the machine.

An alternative flux-based method that could have a more practical feasibility would rely on the analysis of the motor stray flux. In this regard, the study of the external magnetic field in the vicinity of the motor has been proposed as a very interesting alternative for the diagnosis of several motor faults, namely: adjacent rotor faults [17]-[19], eccentricities [20]-[21], stator faults [22]-[24] or even gearbox problems [25]. It has been proven that, when certain faults are present, specific harmonics are amplified in the Fourier spectra of the *Electromotive Force (EMF)* signals induced in external coil sensors installed at different positions. The simplicity, low cost, and easy implementation of the technique makes it a very interesting option to complement the information obtained with other well-known technologies, especially considering the progressive reduction in price of the available flux sensors that comes together with an increase of their features [26]. Though most of the previous works related to flux monitoring have explored the applicability of the technique under stationary conditions, some recent works have also studied the viability of the method under transient operation, obtaining very promising results [27]-[29].

In spite of all these advances, very few works have deepened in the application of the stray-flux analysis technique to detect nonadjacent broken bars in induction motors. One of the few available papers in this topic is [30], which relies on the extraction of certain spectral flux

component over time. Once again, the main constraint is that it focuses on the amplitudes of high order harmonics that may not always be easily detectable.

In this work, a new algorithm to detect rotor damages, in induction motors based on the analysis of stray flux signals is proposed. It uses a spectral pattern recognition method based on the spectral subtraction of the power spectrum of the captured flux signals. The proposed algorithm is applied not only to detect adjacent bar breakages, but also nonadjacent broken bars. In the paper, different positions of the considered sensor are assessed. The results, which are an extension of those already presented in [31], show the potential of this approach, which provides valuable information to detect nonadjacent rotor damages. One important advantage of the proposed approach, in comparison with other methods, is its simple implementation and practical feasibility, since only one sensor measurement is required. Moreover, this can be done in a non-invasive way, without perturbing the operation of the machine. This is a crucial advantage in industry, where non-invasive nature and simplicity are crucial requirements for the massive penetration of fault diagnosis techniques. Finally, the method relies on clear variations of the detected patterns which are discernible even for low fault severity levels and that are based on the overall flux spectrum rather than on particular harmonics that could be easily affected by other phenomena or which may have reduced amplitudes. The validity of the proposed approach is proven through several experimental tests that have been developed with the aid of an in-house built sensor that enables to measure the necessary quantity in a simple and fast way.

## II. ROTOR BAR BREAKAGE DETECTION VIA ANALYSIS OF FLUX SIGNALS

Different authors have proven that the presence of certain faults in the motor amplifies some components in the stray flux spectrum [17]-[25], [32]. Most of these works proposed the use of external coil sensors for the capture of the necessary signals and the subsequent Fourier analysis of these signals to detect the components amplified by rotor damages and other faults. Regarding the detection of bar damages, in [32] it is suggested the study of the sideband components appearing at  $f \cdot (1 \pm 2 \cdot s \cdot f)$  (with  $s$  stands for the *slip* and  $f$  for the supply frequency) around the main frequency component in the FFT spectrum of the captured EMF signals. More recent works such as [17], [33] propose the study of other components in the low frequency region of the FFT spectrum of the EMF induced in external coil sensors; according to these authors, when rotor faults are present, the components located at  $s \cdot f$  and  $3 \cdot s \cdot f$  are amplified in that FFT spectrum. Therefore, the study of the amplitudes of these harmonics may become a reliable indicator of the presence of the fault.

Although most of the works developed in the literature are focused on the analysis of the EMF signals induced in external coil sensors at steady-state operation of the motor, some recent papers have explored the viability of the analysis

of these signals under the startup, obtaining very promising results [27]-[28], [34]. These works have proven that, during transient operation, the fault components follow particular trajectories that can be used as evidences of the failure.

The present work focuses on the flux-based detection of rotor faults but considering the case of nonadjacent broken bars. As commented above, despite several works have stated the difficulties that conventional methods have under this situation, very few works have tried to proposed effective solutions to the problem.

### III. PROPOSED ALGORITHM

To try to achieve some recognition criteria to classify the damages, a method based on the spectrum descending order is applied to the signal obtained after preprocessing (output signal after noise reduction). Later, a spectral subtraction operation with respect to the signal of the healthy motor is also performed [35], [36]. Finally, a moving average block is used as a smoothing filter to eliminate impulsive components of the spectral subtraction. The resulting algorithm given by these processes is described in Fig. 1.

The pattern recognition algorithm is based on the use, as a basic pattern, of the signal of the healthy motor. This is not a serious restriction under a practical point of view, since that signal could be obtained after motor commissioning or after motor inspection, once the rotor is guaranteed to be healthy. In the method, once the actual samples have been captured, they can be compared with the healthy ones. The proposed method is based on searching for patterns, by looking at the differences in the spectrum of both signals (actual sample vs. healthy one). The use of the signal of the healthy motor as a signal reference is analogous to the schemes of adaptive systems. What is obtained at the output is a spectral pattern that identifies the number of broken bars present in the motor.

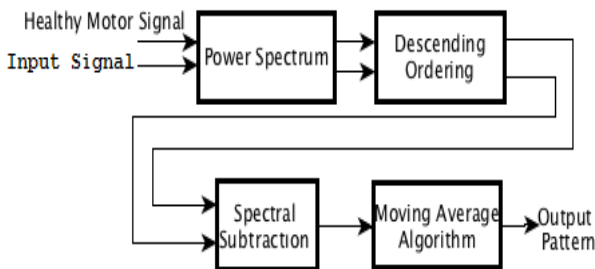


Fig. 1. Block Diagram of the proposed algorithm for identifying broken bars.

For finite duration discrete-time signals  $\{x(n)\}_{n=0}^{N-1}$  (which represents the signal to be processed) and  $\{y(n)\}_{n=0}^{N-1}$  (which represents the healthy motor signal that is taken as reference signal), both of length  $N$  samples, the classic method for estimation of the power spectrum is the periodogram. The periodogram is defined as:

$$P_{xx}(f) = \frac{1}{N} \left| \sum_{m=0}^{N-1} x(m) e^{j2\pi f m} \right|^2 = \frac{1}{N} |X(f)|^2 \quad (1)$$

In our case, the algorithm is based on performing the power spectrum for both signals, namely: the input signal  $x$  and the reference signal  $y$ . Afterwards, we proceed to sort

the power spectrum using descend method. The obtained results for both signals after sorting the power spectrum are used for spectral subtraction. The overall process to perform the proposed algorithm is shown in Fig. 2.

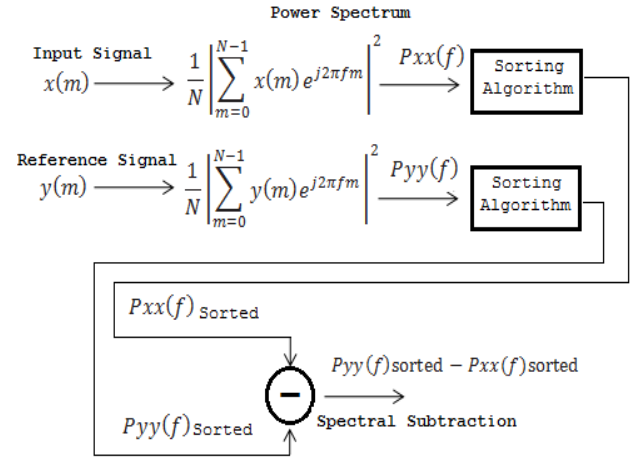


Fig. 2. Method to perform the proposed algorithm.

As a final step, we propose the application of a moving average filter for smoothing.

The novelty of this algorithm relies on the use of a reference signal which controls the entire process, in addition to the use of spectral subtraction and the ordering of the power spectrum. Computational complexity of the algorithm is low, since it is based on second order statistics.

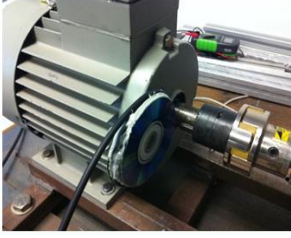
### IV. EXPERIMENTAL RESULTS

Different experiments were developed at the laboratory by using a 4-pole, 1.1 kW induction motor which was coupled to a DC machine acting as a load. The detailed characteristics of the tested motor and load can be found in the Appendix. Different cage rotors (28 bars in each rotor) with diverse levels of failure were available, so that each specific rotor could be assembled to test the corresponding rotor fault condition. More specifically, in this work the considered cases are: healthy rotor and rotor with two broken bars. In this latter case, different relative positions between the broken bars were tested, namely: bars 1-2 broken (adjacent broken bars), bars 1-3 broken, bars 1-4 broken, bars 1-5 broken and bars 1-6 broken.

In each test, the machine was started until it reached the steady-state regime. The EMF signal induced in an external coil sensor attached to the frame of the machine was captured using a digital YOKOGAWA DL-850 oscilloscope. The flux sensor was built in the laboratory and was based on a coil with 1000 turns with an external diameter of 80mm and an internal diameter of 39mm. Two different sensor locations were considered: position A (sensor attached to the lateral part of the motor frame, in the shaft side, Fig. 3 (b)) and position B (sensor attached to the center of the frame, Fig. 3(c)). The signals were captured using a sampling rate of 5 kHz and the acquisition time for the steady-state signals was 40 seconds. Both the experimental test bench and the two considered sensor positions are shown in Fig. 3.



(a)



(b)



(c)

Fig. 3. a) Experimental test bench, b) Position A of the coil sensor, c) Position B of the coil sensor

In order to detect the corresponding faulty condition, the idea of the proposed algorithm to identify the broken bar pattern is to take, as a reference, the healthy state of the motor. The objective is to detect differences in the power spectrum, taking into account that a motor in a healthy state will have a certain power spectrum. When the motor is faulty, it will no longer have the same spectrum. Hence, our method will be based on the rearrangement of the power spectrum and spectral subtraction to obtain an identification pattern of broken bars regardless of the relative position of the bars.

The developed algorithm was conditioned by two goals: 1) it should be able to distinguish between healthy and faulty cases based on the analyses of flux data, and 2) it should be able to detect the existence of the fault regardless of the position of the bars that break.

#### A. Experimental results obtained from the measurement in position A

Regarding the position A, the resulting pattern obtained for each sample after the application of the proposed algorithm (see Fig. 1) allows us to discern when we are in the presence of a motor with two broken bars, since all the samples converge to the same line (see Fig. 4).

In Fig.4 we can also see the stepped positioning of the obtained patterns from each sample according to the relative positions, whose difference lies in the amplitude, that is: first position\_1\_2 (red), position\_1\_6 (black), position\_1\_5 (yellow), position\_1\_3 (green), the above except for position\_1\_4 (blue) which reflects a total difference with the rest of the obtained patterns, from each sample. This result can be very useful for discrimination between the healthy and faulty cases and for the identification of the two broken bars case, regardless of the relative position of the broken bars.

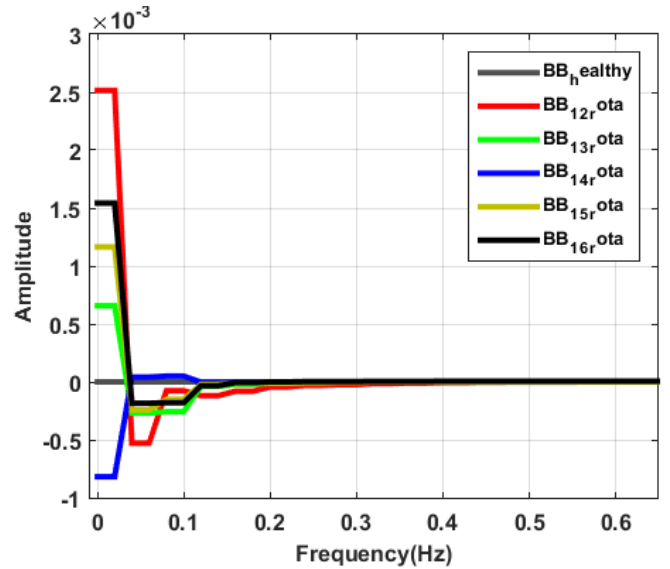


Fig. 4. Resulting spectral pattern obtained from position A.

To prove that we are in the presence of a motor with two broken bars, the Pearson correlation coefficient was applied between the resulting patterns obtained from the measurements carried out in position A. The correlation obtained between the resulting patterns is almost 1, except on the case of position 1\_4. Table I shows the results obtained. In that table, CORR\_POS\_X\_X is the correlation obtained from each pattern with respect to the resulting pattern of the bar BB\_1\_2. The measurement BB\_1\_2 was taken as reference, but another sample could have been taken, the correlation will give similar values with the exception of position 1\_4, which has a certain difference as shown in the graph of Fig.4. Now if we consider the mean value of the module of the obtained correlations, it gives as result: 0.9768.

TABLE I  
CORRELATION VALUES OBTAINED ACCORDING TO THE RESULTING PATTERNS. POSITION A

CORR_POS_1_2 & 1_6 =	CORR_POS_1_2 & 1_5 =
1.0000 0.9933 0.9933 1.0000	1.0000 0.9945 0.9945 1.0000
CORR_POS_1_2 & 1_3 =	CORR_POS_1_2 & 1_4 =
1.0000 0.9344 0.9344 1.0000	1.0000 -0.9849 -0.9849 1.0000

#### B. Experimental results obtained from the measurement in position B

As for the position B, it is verified by the resulting pattern (see Fig.5) that there are two broken bars and just as in the position A, we can discern in which relative position is the position 1\_4 (blue) and the position 1\_6 (black) which are differentiable from the rest of the others, since their correlation value is negative as well as the results of the measurement at position A.

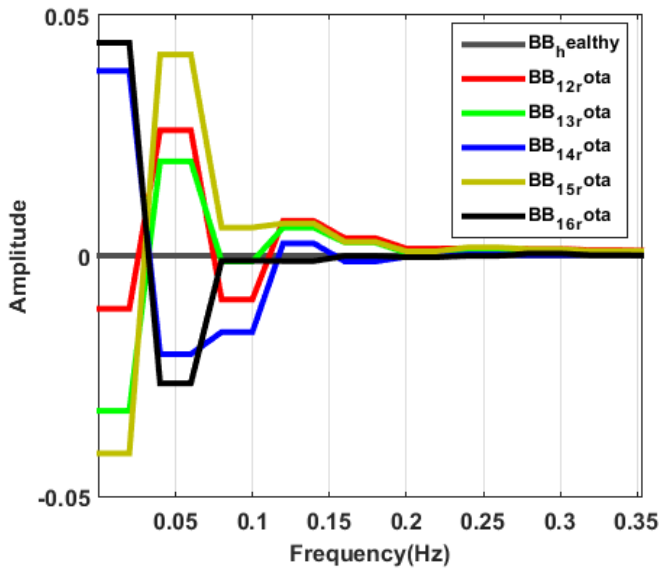


Fig. 5. Resulting spectral pattern obtained from position B.

With respect to the other broken bar relative positions (1\_2, 1\_3 and 1\_5), these follow a stepped descendent pattern as in Fig.2, although not in the same order. The correlation obtained between the resulting patterns as in position A is almost 1, except on the position 1\_4 and position 1\_6, whereby these two positions can be discerned. In Table II the results are shown. Now, if we proceed in the same way as for position A, with the average value of the module of the correlations obtained, it yields: 0.7309. The correlation levels obtained in the measurements made in both relative positions A and B, respectively, oscillate between 0.7 and 0.98, which can be a variable indicator to identify broken bars using the flux signals.

TABLE II  
CORRELATION VALUES OBTAINED ACCORDING TO THE RESULTING PATTERNS. POSITION B

CORR_POS_1_2 & 1_6 =	CORR_POS_1_2 & 1_5 =
1.0000 -0.7361	1.0000 0.8457
-0.7361 1.0000	0.8457 1.0000
CORR_POS_1_2 & 1_3 =	CORR_POS_1_2 & 1_4 =
1.0000 0.7875	1.0000 -0.5542
0.7875 1.0000	-0.5542 1.0000

Note that the power spectra of Figs. 4 and 5 have been sorted according to the amplitude in descending form, as a way to organize the vector to evaluate the spectral subtraction, whose objective is to obtain differences in the spectrum in relation to the healthy state. By carrying out the spectral subtraction of the spectra, only the components in the failure bands will remain, since the components of fundamental frequencies as well as the noise that may exist in the spectrum are cancelled out.

The fault components appear in the spectrum in the bands adjacent to the fundamental frequency. When the spectrum is sorted, the frequency components are placed in descending order according to their amplitude value; the amplitude values of the components where there is a fault will take a new position in the new ordered amplitude vector, but this information is not relevant, since what is

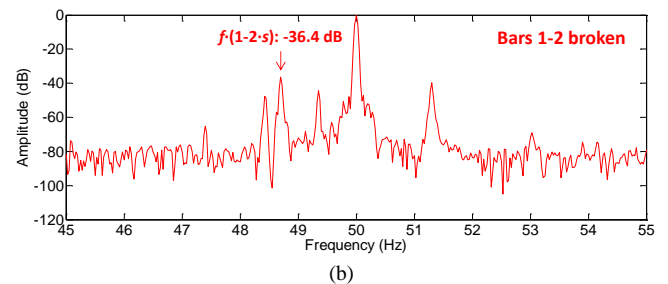
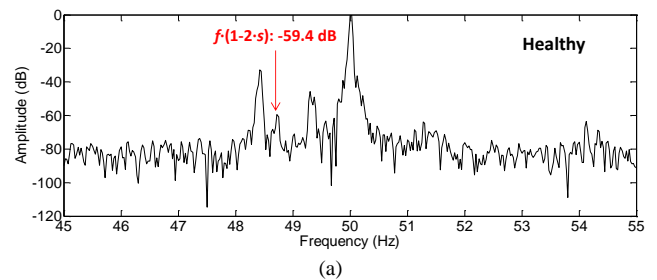
intended is to find out a common pattern for when there are two broken bars, regardless of their relative position, so, in this case, the information relative to the location in the frequency domain is not so relevant.

### C. Discrimination between healthy and damaged state based on the spectra.

The discrimination between healthy and faulty conditions can be carried out by comparing the corresponding spectra of the captured EMF signals. However, this procedure is influenced by the occurrence of nonadjacent breakages since, depending on the relative positions between the bars that break, the amplitudes of the fault harmonics may sensibly differ [30]. However, as pointed out in previous works [17], [33], the analyses of the Fourier spectra may be helpful at least to have an evidence that an anomaly may be present. A rough analysis of the characteristics of the Fourier spectra for each one of the considered positions of the sensor (see Figs 6 and 7) is presented below. Table III synthesizes the conclusions of both figures and includes the case of a single broken bar for comparison purposes.

Characteristics of the spectra for position A:

- All the analyses show the presence of the main rotor fault component (lower sideband harmonic, LSH), which is typically used for diagnosing the fault and that is located at  $f \cdot (1-2 \cdot s)$ . However, note that there are clear differences between the amplitude of this harmonic for healthy and faulty conditions, a fact that may enable to discriminate between both conditions (see Fig. 6).
- Note that, for the different cases of broken bars, the amplitude of the lower sideband harmonic significantly changes. The maximum amplitude is reached when the broken bars are consecutive (positions 1-2), whereas the minimum amplitudes happen when the broken bars are at positions 1-4 and 1-5. This fact clearly confirms the influence of the relative position of the broken bars on the fault component amplitude. In any case, in spite of these differences between faulty cases, the differences are evident versus healthy condition.



[33]. Once again their amplitudes are influenced by the relative positions of the breakages. But their presence is an evidence of the existence of the fault.

In conclusion, the analyses of the spectra can enable to distinguish visually between healthy and faulty conditions but the influence of the relative position between broken bars may make the discrimination difficult in some cases. Due to this, the algorithm proposed in the first part of the paper can be especially useful to diagnose this situation and avoid false negative indications.

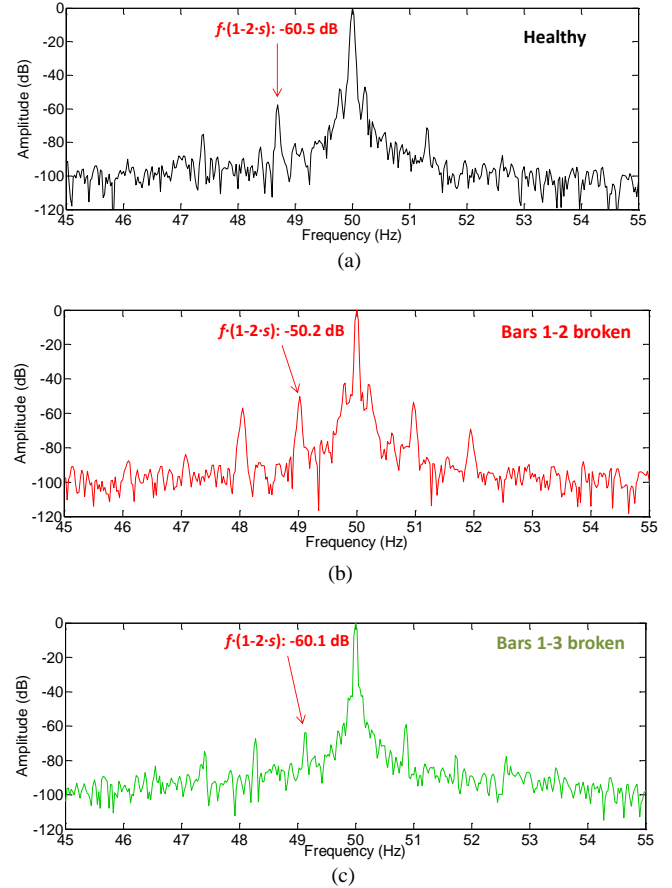
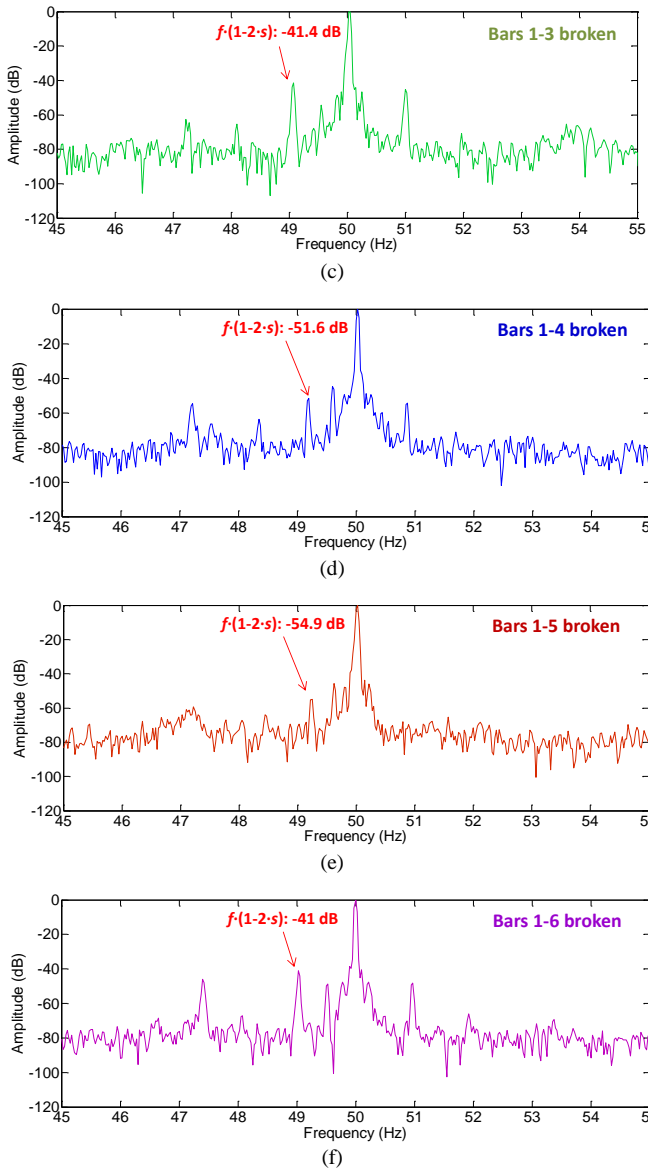
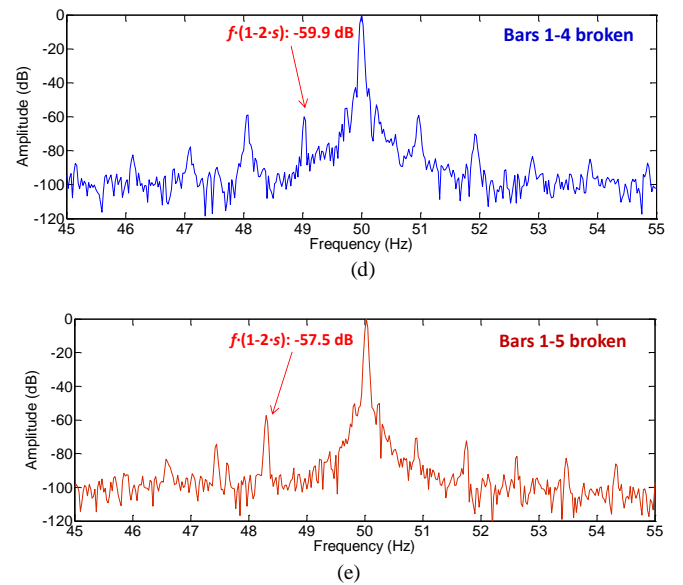


Fig. 6. Comparison of the spectrum of the healthy motor (a), with the broken bars spectra ((b) to (f)). Sensor Position: A

#### Characteristics of the spectra for position B:

- All samples have the expected fundamental harmonic at 50Hz (see Fig. 7).
- As in position A, sideband components are present for all faulty cases although their amplitudes vary depending on the relative position between broken bars (maximum amplitude for adjacent bars, in agreement with the conclusions of previous works focused on current analysis [12]).
- Again, there is a significant variation between the lower sideband amplitude for the faulty cases. In some relative positions, the compensation effect between both breakages may lead to very low amplitudes of the sideband that may lead to difficulties for discriminating versus healthy condition.
- If the low frequency regions (not shown in the figures due to space restrictions) are studied, fault harmonics are detectable at components  $s \cdot f$  and  $3s \cdot f$



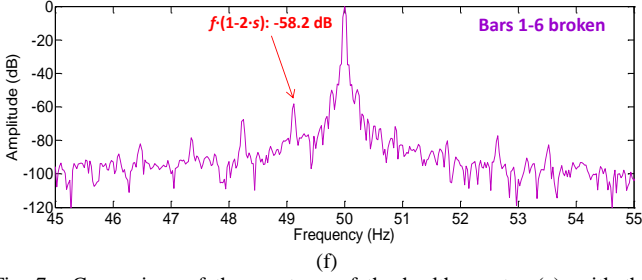


Fig. 7. Comparison of the spectrum of the healthy motor (a), with the broken bars spectra (b) to (f). Sensor Position: B

TABLE III  
LSH FREQUENCY AND AMPLITUDE FOR EACH TESTED  
CONDITION AND FOR EACH SENSOR POSITION

SENSOR POSITION A			
CONDITION	SPEED (RPM)	LSH FREQUENCY (HZ)	LSH AMPLITUDE (DB)
Healthy	1481	48,73	-59,4
1 broken bar	1480	48,67	-53,2
2 broken bars (1-2)	1480	48,67	-36,4
2 broken bars (1-3)	1487	49,13	-41,4
2 broken bars (1-4)	1488	49,20	-51,6
2 broken bars (1-5)	1488	49,20	-54,9
2 broken bars (1-6)	1486	49,07	-41
SENSOR POSITION B			
CONDITION	SPEED (RPM)	LSH FREQUENCY (HZ)	LSH AMPLITUDE (DB)
Healthy	1480	48,67	-60,5
1 broken bar	1486	49,07	-54,1
2 broken bars (1-2)	1484	48,93	-50,2
2 broken bars (1-3)	1488	49,20	-60,1
2 broken bars (1-4)	1485	49,00	-59,9
2 broken bars (1-5)	1479	48,60	-57,5
2 broken bars (1-6)	1486	49,07	-58,2

#### D. Discrimination between healthy and damaged state based on the autocovariance function.

From the previous results based on the information of the frequency spectrum, differences between both spectra can be visually appreciated for the healthy and damaged state. However, it is convenient to obtain an indicator that emits a constant or a variable value in a certain range when it is in the presence of a healthy motor and when the motor is damaged.

In relation to this, in this section an algorithm based on the square value of the median of the autocovariance of the flux signal is proposed. It is decided to use the median and not the mean value so that the amplitude peak in the flux signal has no influence at the time of the calculation of the indicator. The reason for using the quadratic value of the median of the autocovariance is explained by the fact that it is necessary to obtain a quantitative indicator which clearly differs between healthy and faulty conditions. Although other quantities such as the mean value, quadratic mean of variance have been also evaluated, they have not led to so sensitive results as the proposed quantity.

The theoretical foundations of the proposed algorithm are described below: For a stationary periodic real signal, the autocovariance function of a random, stationary process  $\{x(n)\}_{n=0}^{N-1}$  is a measure of the dispersion of the process around its mean value and is defined as a function dependent

on the first and second order moments as follows:

$$c_2^x(\tau) = m_2^x(\tau) - (m_1^x)^2 \quad (2)$$

where  $m_2^x(\tau_1)$  is the autocorrelation function. From the above equation it can be noted that if the process is of value zero mean value, the autocovariance coincides with the autocorrelation function. Then replacing in (2) and applying second order statistics we have:

$$c_2^x(\tau) = \frac{1}{N} \sum_{t=0}^{N-1-\tau} x(t) \cdot x(t + \tau) \quad (3)$$

Then, after obtaining the autocovariance function, we proceed to calculate the square value of the median, for each sample used in the experiment, which is as follows:

Let  $x_1, x_2, x_3, \dots, x_n$  be the data of a sample ordered in increasing order and designating the median  $M_e$  as: if  $n$  is odd, the median is the value occupied by the position

$M_e(c_2^x) = \frac{c_2^x(\tau)_{(n+1)}}{2}$ , then if  $n$  is not odd, the median is the arithmetic mean of the two central values. Then it would be:

$$M_e(c_2^x) = \frac{c_2^x(\tau)_{(\frac{n}{2})} + c_2^x(\tau)_{(\frac{n}{2}+1)}}{2}$$

Substituting to find out the temporary indicator:

$$Ind_t = (M_e(c_2^x))^2 \quad (4)$$

The obtained results applying the proposed algorithm as a temporary indicator for the detection of the healthy-damaged state of the motor are shown in Fig. 8, likewise these are summarized in Table IV.

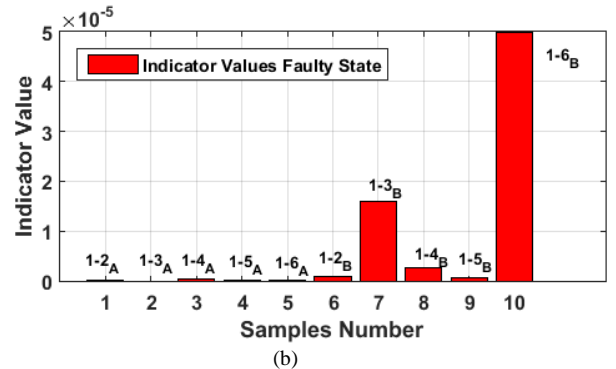
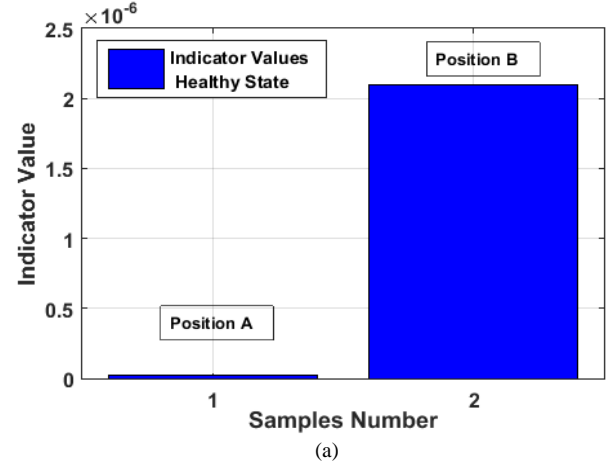


Fig. 8. Comparison between: (a) Indicator for healthy state condition for both sensor positions A and B (b) Indicator for broke state condition for both sensor positions A and B.

TABLE IV  
VALUES OF THE INDICATOR AND MULTIPLICATION FACTOR FOR BOTH  
SENSOR POSITIONS A AND B

SENSOR POSITION	INDICATOR FOR FAULTY STATE	INDICATOR FOR HEALTHY STATE	MULTIPLICATION FACTOR
HEALTHY_A		2.7E-08	
1-2_A	6.8E-09		0.2519
1-3_A	1.7E-10		0.0063
1-4_A	4.4E-07		16.2963
1-5_A	3.4E-09		0.1259
1-6_A	4.65E-08		1.7222
HEALTHY_B		2.1E-06	
1-2_B	9.77E-07		0.4652
1-3_B	1.6E-05		7.6190
1-4_B	2.67E-06		1.2714
1-5_B	5.23E-07		0.2490
1-6_B	5E-05		23.8095

As it can be observed in Table IV, there is a notable difference in the values of the indicator obtained for the position A with respect to those obtained for the position B, even for the same condition. This indicates that the sensor position plays an important role. Note also that there are important differences between the value of the indicator for healthy condition and its corresponding value for each fault condition (second and third columns). In order to obtain a measure of this difference, a multiplication factor is introduced (see fourth column); it is defined as the ratio between the value of the indicator for the corresponding faulty condition and its value for healthy state. This ratio gives an idea of the fault severity in comparison with the healthy condition.

Note that the relative positions 1-3\_A, 1-3\_B and 1-6\_B respectively are the positions where more noticeable differences of the indicator are obtained in relation to the values obtained for the healthy condition. For the other relative positions the differences are not so clear, a fact that indicates that, in addition to the sensor position, the relative position of the broken bar also has certain influence in the results.

## V. CONCLUSIONS

This work proposes the use of induction motor stray flux signals for the identification of bar breakages regardless of their relative position. During the experiments carried out, it was shown that it is possible with the proposed algorithm to detect the fault and even distinguish the relative position of the bars that break.

The proposed method is based on the frequency spectral subtraction of the power spectrum and on the subsequent computation of the Pearson correlation coefficient, which was calculated to demonstrate the similarity of all the patterns obtained for the case of two broken bars [37]-[38].

In order to identify between healthy and damaged state, a rough analysis of the power spectrum may be sufficient in some situations; the differences between the spectrum of the healthy motor and the faulty states in both positions A and B

can be noticed visually, by means of the harmonics appearing both at lower frequencies and around the main component.

Furthermore in relation to this, a potential indicator to evaluate the condition of the motor and discriminate between healthy and damaged state has been evaluated experimentally. This indicator is based on the calculation of the square value of the median of the autocovariance function of the stray flux signal. It is shown that there are quantitative differences in the obtained values when evaluating the indicator for both states(healthy and faulty) and it was demonstrated that the position of the flux sensor as well as the relative position of the broken bar may have influence at the time of calculation of the indicator. According to the obtained results the indicator evaluated when the sensor is at position B seems to be more sensitive than when the sensor is at position A.

## APPENDIX

TABLE V  
RATED CHARACTERISTICS OF THE TESTED MOTOR

Model 1LA2080-4AA10	
Rated power ( $P_N$ )	1.1 kW
Rated speed ( $n_N$ )	1410 rpm
Rated voltage ( $U_N$ )	400(Y)/230 ( $\Delta$ )
Rated current ( $I_N$ )	2.7(Y)/4.6 ( $\Delta$ )
Rated power factor ( $\cos \varphi$ )	0.8
Number of rotor bars	28

TABLE VI  
RATED CHARACTERISTICS OF THE LOAD (D.C.MACHINE)

Rated power ( $P_N$ )	3 kW
Rated speed ( $n_N$ )	2000 -3000 rpm
Rated voltage ( $U_N$ )	220 V
Rated excitation current	0.4 A
Rated armature current	13.6 A
Number of pole pairs	1

## VI. REFERENCES

- [1] S. Nandi, H. A. Toliyat, and Xi. Li, "Condition Monitoring and Fault Diagnosis of Electrical Motors—A Review", *IEEE Transactions on Energy Conversion*, vol. 20, no. 4, pp:719-729, December 2005.
- [2] M. Riera-Guasp, J.A. Antonino-Daviu, and G.A. Capolino, "Advances in Electrical Machine, Power Electronic, and Drive Condition Monitoring and Fault Detection: State of the Art", *IEEE Transactions on Industrial Electronics*, Vol. 62, No. 3, pp:1746-1759, March 2015
- [3] J. A. Antonino-Daviu, M. Riera-Guasp, J. R. Folch, and M. Pilar Molina Palomares, "Validation of a new method for the diagnosis of rotor bar failures via wavelet transform in industrial induction machines," *IEEE Trans. Ind. Appl.*, vol. 42, pp. 990-996, 2006.
- [4] C. Yang, T-J. Kang, D. Hyun, S. Lee, J. Antonino-Daviu, J. Pons-Llinares, "Reliable Detection of Induction Motor Rotor Faults Under the Rotor Axial Air Duct Influence," *IEEE Trans. Ind. Appl.*, vol. 50, no. 4, pp. 2493-2502, Jul.-Aug. 2014.
- [5] J. A. Antonino-Daviu, J. Pons-Llinares, Sungsik Shin, Kun Wang Lee and Sang Bin Lee, "Reliable detection of induction motor rotor faults under the influence of rotor core magnetic anisotropy," in Proc. of the 2015 IEEE 10th International Symposium on Diagnostics for Electrical Machines, Power Electronics and Drives (SDEMPED), Guarda, 2015, pp. 14-21.
- [6] C. Hargis, B. G. Gaydon, and K. Kamash, "The detection of rotor defects in induction motors," in *Proc. 1982 IEE Int. Conf. Electr. Mach., Des. Appl.*, London, U.K., pp. 216-220.

- [7] M. H. Benbouzid, "A review of induction motors signature analysis as a medium for fault detection," *IEEE Trans. Ind. Electron.*, vol. 47, no. 5, pp. 984–993, Oct. 2000.
- [8] T. J. Sobczyk, W. Maciolek, "Does the component  $(1-2s)f_0$  in stator current is sufficient for detection of rotor cage faults?", Proc. SDEMPED 2005, Vienna, Austria, pp. 1-5, Sep. 2005.
- [9] J. Faiz and B. M. Ebrahimi, "Locating rotor broken bars in induction motors using finite element method," *Energy Convers. Manage.*, vol. 50, no. 1, pp. 125–131, Jan. 2009.
- [10] G. Y. Sizov, A. Sayed-Ahmed, C. C. Yeh and Nabeel A. O. Demerdash, "Analysis and Diagnostics of Adjacent and Nonadjacent Broken-Rotor-Bar Faults in Squirrel-Cage Induction Machines," *IEEE Trans. Ind. Elec.*, Vol. 56, No. 11, pp. 4627–4641, Nov. 2009.
- [11] A. Menacer, S. Moreau, G. Champenois, M. S. N. Said, and A. Benakcha, "Experimental detection of rotor failures of induction machines by stator current spectrum analysis in function of the broken rotor bars position and the load," in *Proc. Int. Conf. Comput. Tool*, Sep. 2007, pp. 1752–1758.
- [12] M. Riera-Guasp, M. F. Cabanas, J. A. Antonino-Daviu, M. Pineda-Sánchez and C. H. R. García, "Influence of Nonconsecutive Bar Breakages in Motor Current Signature Analysis for the Diagnosis of Rotor Faults in Induction Motors," in *IEEE Transactions on Energy Conversion*, vol. 25, no. 1, pp. 80–89, March 2010.
- [13] M. Riera-Guasp, J. Pons-Llinares, F. Vedreño-Santos, J. A. Antonino-Daviu and M. Fernández Cabanas, "Evaluation of the amplitudes of high-order fault related components in double bar faults," *8th IEEE Symposium on Diagnostics for Electrical Machines, Power Electronics & Drives*, Bologna, 2011, pp. 307–315.
- [14] J. A. Antonino-Daviu, K. N. Gyftakis, R. Garcia-Hernandez, H. Razik and A. J. M. Cardoso, "Comparative influence of adjacent and non-adjacent broken rotor bars on the induction motor diagnosis through MCSA and ZSC methods," *IECON 2015 - 41st Annual Conference of the IEEE Industrial Electronics Society*, Yokohama, 2015, pp. 1680–1685.
- [15] K. N. Gyftakis, J. A. Antonino-Daviu and A. J. M. Cardoso, "A reliable indicator to detect non-adjacent broken rotor bars severity in induction motors," *2016 XXII International Conference on Electrical Machines (ICEM)*, Lausanne, 2016, pp. 2910–2916.
- [16] C. G. Dias and C. M. de Sousa, "An experimental approach for diagnosis of adjacent and nonadjacent broken bars in induction motors at very low slip," *2017 IEEE International Electric Machines and Drives Conference (IEMDC)*, Miami, FL, 2017, pp. 1–6.
- [17] R. Romary, R. Pusca, J. P. Lecoine, and J. F. Brudny, "Electrical machines fault diagnosis by stray flux analysis," in *Proc. IEEE WEMDCD*, Paris, France, Mar. 11–12, 2013, pp. 247–256.
- [18] A. Yazidi, H. Henao, and G.-A. Capolino, "Broken rotor bars fault detection in squirrel cage induction machines," in *Proc. IEEE IEMDC*, San Antonio, TX, USA, 2005, pp. 741–747.
- [19] H. Henao, G.-A. Capolino, and C. S. Martins, "On the stray flux analysis for the detection of the three-phase induction machine faults," in *Conf. Rec. 38th IEEE IAS Annu. Meeting*, 2003, vol. 2, pp. 1368–1373.
- [20] G. Mirzaeva, K. I. Saad, "Advanced Diagnosis of Rotor Faults and Eccentricity in Induction Motors Based on Internal Flux Measurement", *IEEE Transactions on Industry Applications*, Vol: 54, Issue: 3, pp: 2981 – 2991, May-June 2018.
- [21] S.B. Salem, M. Salah, W. Touti, "Stray Flux analysis for monitoring eccentricity faults in induction motors: Experimental study", In *Control, Automation and Diagnosis (ICCAD)*, 2017 International Conference on, DOI:10.1109/CADIAG.2017.8075673
- [22] L. Frosini, A. Borin, L. Girometta, and G. Venchi, "A novel approach to detect short circuits in low voltage induction motor by stray flux measurement," in *Proc. ICEM*, Marseille, France, Sep. 2–5, 2012, pp. 1538–1544.
- [23] H. Henao, C. Demian, and G.-A. Capolino, "A frequency-domain detection of stator winding faults in induction machines using an external flux sensor," *IEEE Trans. Ind. Appl.*, vol. 39, no. 5, pp. 1272–1279, Sep./Oct. 2003.
- [24] A. Yazidi *et al.*, "Detection of stator short-circuit in induction machines using an external leakage flux sensor," in *Proc. IEEE ICIT*, Hammamet, Tunisia, 2004, pp. 166–169.
- [25] S. M. J. Rastegar Fatemi, H. Henao, and G.-A. Capolino, "Gearbox monitoring by using the stray flux in an induction machine based electromechanical system," in *Proc. IEEE MELECON*, Ajaccio, France, 2008, pp. 484–489.
- [26] C. Jiang, S. Li and T. G. Habetler, "A review of condition monitoring of induction motors based on stray flux," *2017 IEEE Energy Conversion Congress and Exposition (ECCE)*, Cincinnati, OH, 2017, pp. 5424–5430.
- [27] J.A. Ramirez-Nunez, J.A. Antonino-Daviu, V. Climente-Alarcón, A. Quijano-López, H. Razik, R.A. Osornio-Rios, R. de J. Romero-Troncoso "Evaluation of the Detectability of Electromechanical Faults in Induction Motors Via Transient Analysis of the Stray Flux," in *IEEE Transactions on Industry Applications*, vol. 54, no. 5, pp. 4324–4332, Sept.-Oct. 2018.
- [28] H. Cherif, A. Menacer, R. Romary and R. Pusca, "Dispersion field analysis using discrete wavelet transform for inter-turn stator fault detection in induction motors," *2017 IEEE 11th International Symposium on Diagnostics for Electrical Machines, Power Electronics and Drives (SDEMPED)*, Tinos, 2017, pp. 104–109.
- [29] J.A. Antonino-Daviu, H. Razik, A. Quijano-Lopez and V. Climente-Alarcon, "Detection of rotor faults via transient analysis of the external magnetic field," *IECON 2017 - 43rd Annual Conference of the IEEE Industrial Electronics Society*, Beijing, 2017, pp. 3815–3821.
- [30] P. A. Panagiotou, I. Arvanitakis, N. Lophitis, J. A. Antonino-Daviu and K. N. Gyftakis, "Analysis of Stray Flux Spectral Components in Induction Machines under Rotor Bar Breakages at Various Locations," *2018 XIII International Conference on Electrical Machines (ICEM)*, Alexandroupoli, 2018, pp. 2345–2351.
- [31] M. E. Iglesias-Martínez, P. F. de Córdoba, J. A. Antonino-Daviu and J. A. Conejero, "Detection of Bar Breakages in Induction Motor via Spectral Subtraction of Stray Flux Signals," in *2018 XIII International Conference on Electrical Machines (ICEM)*, Alexandroupoli, Greece, 2018, pp. 1796–1802.
- [32] A. Bellini, C. Conconi, G. Franceschini, C. Tassoni and A. Toscani, "Vibrations, currents and stray flux signals to assess induction motors rotor conditions", *IECON 2006 - 32nd Annual Conference on IEEE Industrial Electronics*, Paris, 2006, pp. 4963–4968.
- [33] A. Ceban, R. Pusca and R. Romary, "Study of Rotor Faults in Induction Motors Using External Magnetic Field Analysis", *IEEE Trans. Ind. Electronics*, vol. 59, no. 5, pp. 2082–2093, 2012.
- [34] J.A. Antonino-Daviu, H. Razik, A. Quijano-Lopez and V. Climente-Alarcon, "Detection of rotor faults via transient analysis of the external magnetic field," *IECON 2017 - 43rd Annual Conference of the IEEE Industrial Electronics Society*, Beijing, 2017, pp. 3815–3821.
- [35] K. C. Deekshit Kompella, M. Venu Gopala Rao, R. Srinivasa Rao, "SWT based bearing fault detection using frequency spectral subtraction of stator current with and without an adaptive filter", *TENCON 2017 - 2017 IEEE Region 10 Conference Electronic ISSN: 2159-3450*, DOI: 10.1109/TENCON.2017.8228277.
- [36] El Houssin, El Bouchikhi, Vincent Choqueuse, Mohamed El Hachemi Benbouzid, "Current Frequency Spectral Subtraction and Its Contribution to Induction Machines' Bearings Condition Monitoring" *IEEE Transactions on Energy Conversion*, Vol.: 28, Issue: 1, March 2013.
- [37] H. Deborah, N. Richard, and J. Y. Hardeberg, "A Comprehensive Evaluation of Spectral Distance Functions and Metrics for Hyperspectral Image Processing", *IEEE Journal of Selected Topics in Applied Earth Observations and Remote Sensing*, vol. 8, no. 6, June 2015.
- [38] [2] G. Borelli, J. Jovic Bonnet, Y. Rosales Hernandez, K. Matsuda, J. Damerou, "Spectral-Distance-Based Detection of EMG Activity From Capacitive Measurements", *IEEE Sensors Journal*, Vol. 18, Issue: 20 Oct. 15, 2018.

## VII. BIOGRAPHIES



**Miguel Enrique Iglesias Martínez** was born in Pinar del Río Cuba in 1984. He obtained a degree in Telecommunications and Electronics Engineering from the University of Pinar del Río (UPR), in 2008. He obtained a Master's Degree in Digital Systems at the Higher Polytechnic Institute (CUJAE), La Habana, Cuba, in 2011. He has obtained 4 scientific prizes from the Cuba Academy of Sciences in the years 2011, 2012, 2015 and 2017 respectively. He is currently doing his PhD in Mathematics at the Universitat Politècnica de València. His areas of research interest are: Signal Processing, Noise Analysis and Blind Information Extraction, as well as the Design of Digital Systems



**Pedro Fernández de Córdoba** was born in Valencia in October 1965. He obtained the degree, the M.Sc., and the Ph.D. in Theoretical Physics from the Universitat de València (UV), Valencia, Spain in 1988, 1990, and 1992, respectively. He also obtained the Ph.D. in Mathematics from the Universidad Politécnica de Valencia (UPV), Valencia, Spain, in 1997. His research work was performed at UV, UPV, the Joint Institute for Nuclear Research (Russia), the University of Tübingen (Germany) and the Istituto Nazionale di Fisica Nucleare (INFN) in Torino (Italy), among others. He is currently Professor in the Department of Applied Mathematics at UPV. Nowadays, his research interests include the area of modelling and numerical simulation of physical and engineering problems, mainly focusing on the numerical treatment of heat and mass transfer problems. Pedro Fernández de Córdoba is Doctor Honoris Causa from University of Pinar del Rio (Cuba), member of the Colombian Academy of Exact, Physical and Natural Sciences, member of the Académie Nationale des Sciences, Arts et Lettres du Bénin, Profesor Invitado of the University of Pinar del Rio (Cuba) and Profesor Visitante "Ad Honorem" of the Universidad del Magdalena (Colombia). Furthermore, since its establishment on September 30, 2011, he has been member of the Board of the Spanish Mathematics-Industry network ([www.math-in.net](http://www.math-in.net)).



**Jose A. Antonino-Daviu (S'04, M'08, SM'12)** received his M.S. and Ph. D. degrees in Electrical Engineering, both from the Universitat Politècnica de València, in 2000 and 2006, respectively. He also received his Bs. in

Business Administration from Universitat de Valencia in 2012. He was working for IBM during 2 years, being involved in several international projects. Currently, he is Associate Professor in the Department of Electrical Engineering of the mentioned University, where he develops his docent and research work. He has been invited professor in Helsinki University of Technology (Finland) in 2005 and 2007, Michigan State University (USA) in 2010, Korea University (Korea) in 2014 and Université Claude Bernard Lyon 1 (France) in 2015. He is IEEE Senior Member since 2012 and he has published over 170 contributions, including international journals, conferences and books. He is also Associate Editor of IEEE transactions on Industrial Informatics and IEEE IAS Distinguished Lecturer for 2019-20. He has been Guest Editor in IEEE transactions on Industrial Electronics. He was General Co-Chair of IEEE SDEMPED 2013. He received the Nagamori Award from Nagamori Foundation in Kyoto, Japan in 2018, for his contributions in electric motors transient analysis area.



**J. Alberto Conejero** received his degree on Mathematics from Universitat de València (UV), and the Ph.D. degree from Universitat Politècnica de València (UPV), Spain, in 2004, receiving the Outstanding Dissertation Award. He is associate professor at UPV since 2009. He is author of more than 60 papers in international journals. His research interests are dynamical systems, partial differential equations, graph theory, and the multidisciplinary applications of mathematics to computer science, engineering, and biotechnology. He has been invited researcher of Bowling Green St. Univ (USA), Kent St. Univ. (USA), Università del Salento (Italy), Universität Tübingen (Germany), and Czech Academy of Sciences (Czech Rep.). He has been awarded with the Teaching Excellence prize of UPV in 2014. He is currently the Director of the Department of Applied Mathematics, UPV, and responsible of the Msc program on Mathematics Research at UPV.